Articl ID 1004-924X(2003)04-0394-06

Novel stack-shorted microstrip bluetooth antenna

YU Wen-ge, ZHONG Xian-xin, WU Zheng-zhong, LI Xiao-yi

(The Key Lab for Optoelectronic Technology & Systems of Ministry of Education, Chongqing University, Chongqing 400044, China)

Abstract: For the rapid development of bluetooth wireless communication, a novel stack-shorted micromachined bluetooth antenna was designed with a 10 dB bandwidth of more than 11 % and an efficiency of more than 68 %, respectively, the length is less than 1/7 wavelength. The alternating direction implicit finite-difference time-domain (ADI-FDTD) method for a full three-dimensional (3-D) wave is used for modeling and analyzing the antenna for the first time. Numerical simulation results manifest that the ADI-FDTD method is more efficient than the conventional 3-D FDTD method in terms of the central processing unit time if the size of the local minimum cell in the computational domain is much smaller than those of cells or the wavelength. It can efficiently reduce the CPU time.

Key words: bluetooth; ADI-FDTD method; FDTD method; microstrip antenna; MEMS

CLC number: TN820.27 **Document code:** A

新型层叠短接式微带蓝牙天线的仿真分析

余文革,钟先信,巫正中,李晓毅

(重庆大学 光电技术及系统教育部重点实验室, 重庆 400044)

摘要:为适应快速发展的蓝牙无线通信技术的要求,设计了新型层叠短接式微机械蓝牙天线,其 10dB 带宽达到了 11 % 以上,辐射效率为 68 %,天线长度小于 1/7 λ。首次将三维 ADI-FDTD (the alternating direction implicit finite-difference time-domain) 全波分析方法应用于该天线的建模和分析,数值模拟结果表明在计算域内网格尺寸相对于其它处网格尺寸或波长小得多的条件下,三维 ADI-FDTD 时域全波分析方法能更有效地模拟微机械微带蓝牙天线,并能有效地减少 CPU 计算时间。

关 键 词:蓝牙;ADI-FDTD 方法;FDTD 方法;微带天线;微电子机械系统

中图分类号:TN820.27 **文献标识码**:A

1 Introduction

As microwave equipment requires low profile and lightweight to assure reliability, an antenna with these characteristics is essentially required and a microstrip antenna satisfies such requirement. Microstrip antennas have conformal structure, low cost, and ease of integration with

Received date: 2003-03-14; **Revised date**: 2003-05-15.

Foundation item: Project Supported by the Major State Basic Research Development Program "Integrated Micro-Optical-Electronic-Mechanical System" (Project No. G19999033105)

solid-state devices as well as low profile and lightweight. But the microstrip antennas have a narrow bandwidth which is about 0.6～3%. In the last decade, many researchers studied the bandwidth widening technique of microstrip antennas[1-3]. For a serial of salient features, the microstrip antennas are used widely in the communication and other aspects.

The finite-difference time-domain (FDTD) method[4] is widely used for solving problems related to electromagnetism. As the tradition FDTD method is based on an explicit finite-difference algorithm, the Courant-Friedrich-Levy (CFL) condition[5] must be satisfied when this method is used. Therefore, a maximum time-step size is limited by minimum cell size in a computation domain. In this paper, we first adopted the alternating direction implicit finite-difference time-domain (ADI-FDTD) method[6] for a full three-dimensional (3-D) wave to Yee's staggered cell to analyze and simulate the bluetooth antenna. The numerical method is unconditionally stable and is not dissipative. Therefore, time-step size can be arbitrarily set when this method is used. The limitation of the maximum time-step size of the method does not depend on the CFL condition, but rather on numerical errors. Associated with practical model, a kind of approximate absorbing boundary condition was developed. Comparing with the full Si antenna[7], the antenna in this paper has more wider bandwidth and higher efficiency. Numerical results manifest that the 3-D ADI-FDTD method is more efficient than the conventional FDTD method within numerical errors.

2 Stack-shorted microstrip bluetooth antenna

The 2.4 GHz stack-shorted microstrip bluetooth patch antenna is shown in Fig. 1. Because silicon-based micromaching process is compatible with standard IC technology, and prone to integration with other components, silicon wafer (ε_r = 11.7) was selected as a layer of microstrip substrate. Between the ground plate and the wafer there is a layer of air (ε_r = 1), which could suppress surface wave induced in the wafer substrate, as a result, the efficiency and the bandwidth of the antenna were increased, and the radiation pattern improved. A layer of TEFLON (ε_r = 2.3) was sandwiched between the driven and parasitic patch. By adding a passive parasitic patch, which resonates near the central resonant frequency of the driven patch, the bandwidth of the novel antenna was further extended.

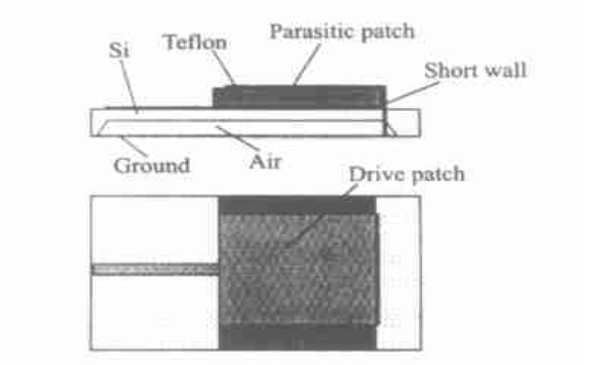

Fig. 1 Stacked bluetooth antenna

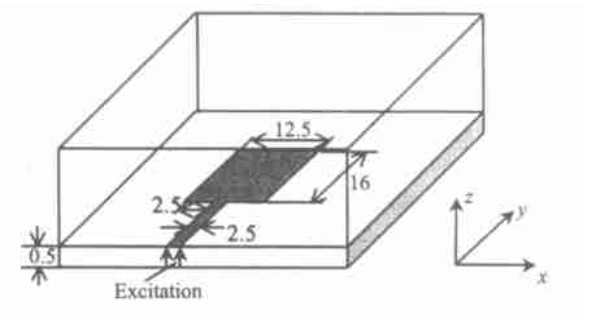

Fig. 2 Bluetooth antenna and its calculation domain

3 3-D ADI-FDTD algorithm

3.1 Numerical formulations of the 3-D ADI-FDTD method

For E_x component, the numerical formulation of the ADI-FDTD method for a full 3-D wave is presented as follows. The electromagnetic field components are arranged on the cells in the same way as that using the conventional FDTD method. These formulations are available for homogeneous

lossless medium and for using nonuniform cells. The calculation for one discrete time step is performed using two procedures.

$$E_x^{n+1/2}(i+1/2,j,k) = E_x^n(i+1/2,j,k) + \frac{\Delta t}{\varepsilon}\cdot \{[H_z^n(i+1/2,j+1/2,k) - H_z^n(i+1/2,j-1/2,k)]/\Delta y - [H_y^{n+1/2}(i+1/2,j,k+1/2) - H_y^{n+1/2}(i+1/2,j,k-1/2)]/\Delta z\}, \quad (1)$$

$$H_y^{n+1/2}(i+1/2,j,k+1/2) = H_y^n(i+1/2,j,k+1/2) + \frac{\Delta t}{\mu}\cdot\{[E_z^n(i+1,j,k+1/2) - E_z^n(i,j,k+1/2)]/\Delta x - [E_x^{n+1/2}(i+1/2,j,k+1) - E_x^{n+1/2}(i+1/2,j,k)]/\Delta z\}, \quad (2)$$

In this procedure, the component on the left-hand side and the component on the right-hand side are defined as synchronous variables in (1), thus, a modified (1^*) for the E_x component is derived from (1) and (2) by eliminating the $H_y^{n+1/2}$ components. In the suffix k, (1^*) indicates k maximum number of simultaneous linear equations and also means z-directional scan of the E_x components as follows:

$$-\eta_1 E_x^{n+1/2}(i+1/2,j,k-1) + \eta_2 E_x^{n+1/2}(i+1/2,j,k) - \eta_3 E_x^{n+1/2}(i+1/2,k+1) = \frac{\varepsilon}{\Delta t}E_x^n(i+1/2,j,k) + [H_z^n(i+1/2,j+1/2,k) - H_z^n(i+1/2,j-1/2,k)]/\Delta y - [H_y^n(i+1/2,k+1/2) - H_y^n(i+1/2,j,k-1/2)]/\Delta z + \frac{\Delta t}{\mu}[E_z^n(i+1,j,k-1/2) - E_z^n(i,j,k-1/2)]/\Delta x\Delta z - \frac{\Delta t}{\mu}[E_z^n(i+1,j,k+1/2) - E_z^n(i,j,k+1/2)]/\Delta x\Delta z, \quad (1^*)$$

where

$$\eta_1 = \frac{\Delta t}{\mu(\Delta z)^2}, \eta_2 = \frac{\varepsilon}{\Delta t} + \eta_1 + \eta_3, \eta_3 = \frac{\Delta t}{\mu(\Delta z)^2}.$$

In the same way, we can obtain the modified equation for $E_y^{n+1/2}$ and $E_z^{n+1/2}$ component.

$$E_x^{n+1}(i+1/2,j,k) = E_x^n(i+1/2,j,k) + \frac{\Delta t}{\varepsilon}\cdot\{[H_z^{n+1}(i+1/2,j+1/2,k) - H_z^{n+1}(i+1/2,j-1/2,k)]/\Delta y - [H_y^{n+1/2}(i+1/2,j,k+1/2) - H_y^{n+1/2}(i+1/2,j,k-1/2)]/\Delta z\}, \quad (3)$$

$$H_z^{n+1}(i+1/2,j+1/2,k) = H_z^{n+1/2}(i+1/2,j+1/2,k) + \frac{\Delta t}{\mu}\cdot\{[E_x^{n+1}(i+1/2,j+1,k) - E_x^{n+1}(i+1/2,j,k)]/\Delta y - [E_y^{n+1/2}(i+1,j+1/2,k) - E_y^{n+1/2}(i,j+1/2,k)]/\Delta x\}, \quad (4)$$

In the second procedure, the E_x component on the left-hand side and the H_z component on the right-hand side are defined as synchronous variables in (3), thus, a modified (2^*) for the E_x component is derived from (3) and (4) by eliminating the H_z^{n+1} components. In the suffix j, (2^*) indicates j maximum number of simultaneous linear equations and also means y-directional scan of the E_x components as follows:

$$-\phi_1 E_x^{n+1}(i+1/2,j-1,k) + \phi_2 E_x^{n+1}(i+1/2,j,k) - \phi_3 E_x^{n+1}(i+1/2,j+1,k) = \frac{\varepsilon}{\Delta t}E_x^{n+1/2}(i+1/2,j,k) + [H_z^{n+1/2}(i+1/2,j+1/2,k) - H_z^{n+1/2}(i+1/2,j-1/2,k)]/\Delta y - [H_y^{n+1/2}(i+1/2,j,k+1/2) - H_y^{n+1/2}(i+1/2,j,k-1/2)]/\Delta z + \frac{\Delta t}{\mu}[E_y^{n+1/2}(i+1,j-1/2,k) - E_y^{n+1/2}(i,j-1/2,k)]/\Delta x\Delta y - \frac{\Delta t}{\mu}[E_y^{n+1/2}(i+1,j+1/2,k) - E_y^{n+1/2}(i,j+1/2,k)]/\Delta x\Delta y, \quad (2^*)$$

where

$$\phi_1 = \frac{\Delta t}{\mu(\Delta y)^2}, \phi_2 = \frac{\varepsilon}{\Delta t} + \phi_1 + \phi_3, \phi_3 = \frac{\Delta t}{\mu(\Delta y)^2}.$$

the modified equation for E_y^{n+1} and E_z^{n+1} component can be obtained accordingly. By solving these simultaneous linear equations, we can get the values of the electric-field components at the time of $n+1$. Thereafter, we can get the values of the magnetic-field components at

the time of $n + 1$.

3.2 Accuracy and stability

To ensure the accuracy of computed results, the spatial increment must be small compared to the wavelength at the frequency of computation, usually,

$$\max(\Delta x, \Delta y, \Delta z) < \lambda / 10 , \qquad (5)$$

Since the simultaneous linear equations such as (1*) and (2*) can be written in a tridiagonal matrix form, and their coefficients on the left-hand side satisfy strict superiority on the cross. The 3-D ADI-FDTD algorithm is unconditionally stable.

3.3 Setting of absorbing Boundary conditions

The field computation domain must be limited in size because the computer can not store an unlimited amount of data. Several absorbing boundary conditions (ABCs)[8] are developed nowadays. Mur ABCs and superabsorption boundary conditions are used in this paper, respectively.

For different reflection characterization in the direction along which the electromagnetic wave propagates, we will discuss which ABCs should be selected for top, side, front and rear surface individually.

In the rear surface ($k = G$), the first order Mur ABCs are set. Electromagnetic waves are propagated along $+z$ direction, the electronic field component ($E_y = E_z = 0$) satisfies the one-way wave equation

$$\left(\frac{\partial}{\partial z} - \frac{1}{v}\frac{\partial}{\partial t}\right) E_x = 0 , \qquad (6)$$

its finite difference form is

$$E_x^{n+1}(i, j, k) = E_x^n(i, j, G-1) + \frac{v\Delta t - \Delta z}{v\Delta t + \Delta z}\left[E_x^{n+1}(i, j, G-1) - E_x^n(i, j, G)\right], \qquad (7)$$

where v is the phase velocity of electromagnetic wave at the boundary surface. The setting of the other surface are similar to that of the rear surface.

4 Numerical results

For reaching the match of impedance, there are some offsets for microstrip feed-line. In Fig. 2, Let $\Delta x = \Delta y = 0.25$ mm, $\Delta z = 0.125$ mm, the domain of total computation is $60 \times 100 \times 40$. In microwave circuit analysis, Gauss impulse is generally selected as an excitation for smoothness in time domain and easy spectrum width setting. The width of Gauss pulse is $T = 15$ ps, Assume that the time delay $t_0 = 3T = 45$ ps, Electronic filed distribution of micromachine bluetooth antenna at a certain moment are shown in Fig. 3. It is shown that electromagnetic wave is mainly centralized beneath the microstrip transmission line and patch, and propagates along $+z$ direction. In Fig. 3, there is a pulse value of the electronic field near the front surface, it is caused by the tangential electronic field component derived from the magnetic wall condition.

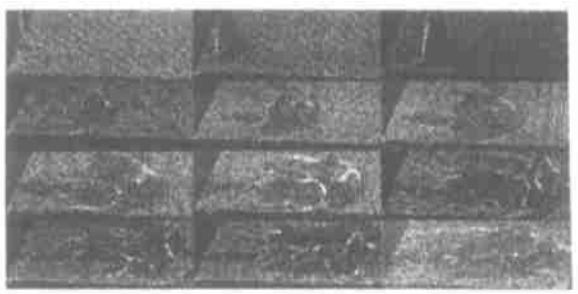

Fig. 3　Electronic field simulation of micromachine bluetooth antenna (t = 15、30、45、60、75、90、105、120、135、150、165、180 time step)

The response value of the frequency domain can be calculated by Fourier-transforming the time domain value. As the microstrip feed-line is an open stub, the microstrip antenna is a 1-port circuit. So the reflection coefficient S_{11} of the microstrip antenna is

$$S_{11} = \frac{F[V_r(t)]}{F[V_i(t)]} , \qquad (8)$$

where $V_r(t)$ is a reflected voltage, $V_i(t)$ is an incident voltage, and F is a Fourier transform. From the calculated reflection coefficient, voltage standing wave ratio (VSWR) can be calculated as

$$\mathrm{VSWR} = \frac{V_{\max}}{V_{\min}} = \frac{1 + |S_{11}(w)|}{1 - |S_{11}(w)|} , \qquad (9)$$

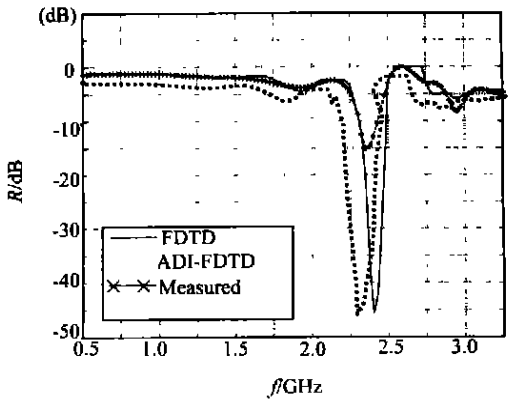

Fig. 4　Return loss of silicon micromachined patch antenna

The percent bandwidth of the antennas was determined from the impedance data. For ease of notion, the bandwidth refers to percent bandwidth which is normally defined as

$$\text{percent BW} = [(f_{r_2} - f_{r_1})/f_r] \times 100\ \%\ , \tag{10}$$

where f_r is the resonance frequency, while f_{r1} and f_{r2} are the frequencies between which reflection coefficient of the antenna is less than or equal to 1/3, which corresponds to VSWR ≤ 2.

The circle wave loss of antenna measured and computed are shown in Fig. 4. from Fig. 4, we can find the computed results by using ADI-FDTD method are in good agreement with the computed results by using FDTD method. The measurements carried out on an Agilent 8720C vector network analyzer show that its resonant frequency is 2.44 GHz, The drift between the design and measured frequencies is less than3 %. the length of the novel patch antenna is only 1/7 wavelength, By using stacked structure, the relative bandwidth of the antenna is approximately 11 %, while that of a conventional microstrip antenna is only 0.6～3 %. The efficiency this novel antenna arrive at 68 %.

The characteristic parameters such as effective dielectric constant, the characteristic impedance in spectrum domain could be worked out by Fourier transition. Through dealing with the computed data using MATLAB, The antenna radiation patterns are shown in Fig. 5.

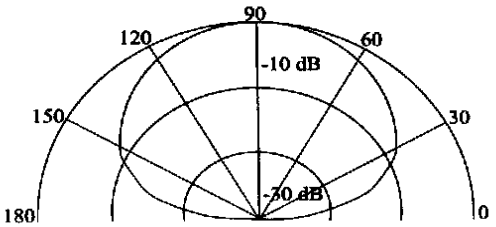

(a) H-plane

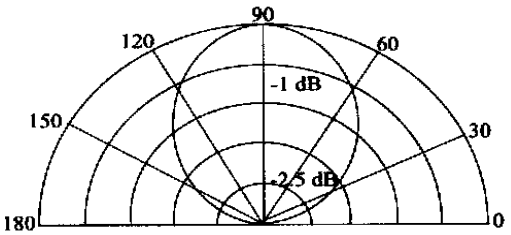

(b) E-plane

Fig. 5　Full wave analysis radiation pattern of micromachined Bluetooth antenna

These simulations were performed by XFDTD, the CPU time of these simulations are shown in Tab. 1, with the time-step size and total time steps. In case of the ADI-FDTD, the time-step size can be set 15 times as large as the conventional FDTD, and total time steps can be reduced by a factor of 15. The CPU time is also reduced to 28.2 %.

Tab. 1　Information on the bluetooth antenna simulation

	Δt	steps	CPU Time
FDTD	0.25 ps	1500	465.2 s
ADI-FDTD	3.75 ps	100	131.3 s

5　Conclusion

A novel stacked microstrip bluetooth antenna has been presented in this paper, it performs excellently especially in miniaturization and bandwidth broadening. it has been proved to suit bluetooth communication.

ADI-FDTD method was used to model the structure of the antenna. The algorithm of the

method is unconditionally stable. Thus, the limitation of the maximum time-step size does not depend on the CFL condition, but rather on numerical errors. The fact that there is a good agreement between the ADI-FDTD computed values and FDTD computed values manifests that the 3-D ADI-FDTD method is more efficient than the conventional FDTD method. It can efficiently reduce the CPU time.

参考文献:

[1] LIU ZH F, KOOI P SH. A Method for designing broad-band microstripAntenna in multilayered planar structures[J]. *IEEE Trans. Antennasand Propagat*, 1999,47(9): 1416-1420.

[2] WU ZH Zh, ZHONG X X, LI X Y, *et al*. Broadband micromachined antenna for Bluetooth device[A]. *ISIST*'2002 [C]. Jinan, China. 18-22, 2002,1(2): 728-732.

[3] WU ZH ZH, ZHONG X X, LI X Y, *et al*. Broadband micromachined Bluetooth antenna[A]. *Pacific Rim Workshop on Micro/ Nano Technologies* [C]. Xiamen, China. 2002,22-24:509-512.

[4] YEE K S. Numerical solution of initial boundary value problems involving maxwell's equations in isotropic media[J]. *IEEE AP*, 1996,14(5):302-307.

[5] TAFLOVE A, BRODWIN M E. Numerical solution of steady state electromagnetic scattering problem using the time dependent maxwell's equations[J]. *IEEE Trans* MTT, 1975,23(8):623-630.

[6] NAMIKI T. A new FDTD algorithm based on alternating direction implicit method[J]. *IEEE Trans Microwave Theory Tech.*, 1999,47(9):2003-2007.

[7] WU Zh ZH, ZHONG X X, LI X Y, *et al*. Multiplayer-shorted micromachined Bluetooth antenna[J]. *Optics and Precision Engineering*. 2001, 9(6):572-576.

[8] MUR G. Absorbing boundary conditions for the finite-difference approximation of the time-domain electromagnetic field equations[J]. *IEEE Trans EMC*, 1981,23(4): 377-382.

作者简介:**余文革**(1967 -),**男**,**四川渠县人**,**重庆大学光电工程学院博士生**,**主要从事** MEMS **天线及电磁场数值分析方面的研究**;

钟先信(1935 -),**男**,**重庆人**,**重庆大学光电工程学院教授**,**博士生导师**,**主要从事精密机械及** MEMS **方面的研究**。